Journal of Pain Research

Dovepress
open access to scientific and medical research

Open Access Full Text Article

ORIGINAL RESEARCH

Decreased expression of lncRNA Malat1 in rat spinal cord contributes to neuropathic pain by increasing neuron excitability after brachial plexus avulsion

This article was published in the following Dove Press journal:
Journal of Pain Research

Chong Meng[1–3]
Xun Yang[1–3]
Yuzhou Liu[1–3]
Yingjie Zhou[1–3]
Jing Rui[1–3]
Shenqian Li[1–3]
Ce Xu[1–3]
Yongqing Zhuang[4]
Jie Lao[1–3]
Xin Zhao[1–3]

[1]Department of Hand Surgery, Huashan Hospital, Fudan University, Shanghai 200040, People's Republic of China; [2]Key Laboratory of Hand Reconstruction, Ministry of Health, Shanghai 200032, People's Republic of China; [3]Shanghai Key Laboratory of Peripheral Nerve and Microsurgery, Shanghai 200032, People's Republic of China; [4]Hand Surgery Department, Shenzhen People's Hospital, Shenzhen 518020, People's Republic of China

Purpose: Neuropathic pain (NP) is a challenging clinical problem due to its complex pathogenesis. In our previous study using microarray, we found that the levels of lncRNA Malat1 were decreased in the spinal cord of NP rat after brachial plexus avulsion, but its contribution to NP remain unclear. The purpose of this study was to investigate its role in the pathogenesis of NP.

Methods: In the NP model of complete brachial plexus avulsion rat, spinal cords were harvested, and fluorescence in situ hybridization (FISH) was used to test the spatial expression of Malat1 and qRT-PCR was used to confirm the quantitative expression of Malat1. In primary cultured neurons, Malat1 expression interfered with adenovirus. Spontaneous electric activities of neurons were tested using multi-electrode arrays and apoptosis of neurons was tested using TUNEL method. The change of intracellular calcium concentration was analyzed using calcium imaging method.

Results: Decreased Malat1 expression was confirmed using qRT-PCR, and Malat1 was identified in the cytoplasm of neurons in spinal cord, but not in glia. In vitro, the decrease of Malat1 resulted in an increase in the frequency of spontaneous electric activity in neurons but had no effect on neuronal apoptosis. Further analysis indicated during glutamate stimulation, the change of intracellular calcium concentration in neurons with downregulated Malat1 expression was significantly greater than that in normal neurons.

Conclusion: Reduced Malat1 expression may induce NP by increasing neuronal excitability in the spinal cord via regulation of calcium flux.

Keywords: neuropathic pain, lncRNA, Malat1, spinal cord, neuron, multielectrode array, brachial plexus avulsion

Introduction

Neuropathic pain (NP), which is defined as "pain arising as a direct consequence of a lesion or disease affecting the somatosensory system" by the NeuPSIG, presents as a kind of refractory pain in the clinic.[1] Brachial plexus avulsion is a severe injury with high incidence of refractory neuropathic pain, which were more than 60% and might reach up to 96% in some serials.[2,3] Limited clinical success has been achieved owing to incomplete understanding of mechanisms underlying NP in brachial plexus injury patients. Brachial plexus avulsion involved the transition area between the central and peripheral nervous system, so did the mechanisms underlying the secondary NP. It was thought that the apoptosis of inhibitory interneurons and the hyperexcitability of sensory neurons in the spinal cord dorsal horn contributed the NP development.[3,4]

Correspondence: Xin Zhao
Department of Hand Surgery, Huashan Hospital, Fudan University, No. 12 Rd. Wulumuqi (M), Jing'an District, Shanghai 200040, People's Republic of China
Tel +861 381 613 1608
Email zhaoxin888@sina.com

submit your manuscript | www.dovepress.com
DovePress
http://doi.org/10.2147/JPR.S195117

Long non-coding RNAs (lncRNAs) are non-coding RNAs longer than 200 nucleotides.[5] Accumulating evidence indicates that lncRNAs possess multiple functions and participate in a wide variety of cellular processes.[6] Zhao et al have reported that lncRNA kcna2-as is downregulated under the control of the transcription factor MZF1 in dorsal root ganglion neurons of NP mice.[7] The spinal cord is responsible for receiving input from nociceptors and projecting these signals to brain after integrating them with signals from descending inhibitory and facilitatory systems.[8] It thus plays an important role in the process of central sensitization. However, whether and how lncRNAs regulate NP in the spinal cord have not yet been reported.

In our previous study using lncRNA microarrays, we determined the lncRNA profile in the spinal cord of rat model of NP after brachial plexus avulsion. We found that lncRNA metastasis-associated lung adenocarcinoma transcript 1 (Malat1) was downregulated significantly in the spinal cord of brachial plexus avulsion-induced NP rats. Here we further investigated the role of Malat1 in the pathogenesis of NP. We found that Malat1 may act as an active regulator in the pathogenesis of brachial plexus avulsion-induced NP by inducing abnormal excitability of neurons via regulation of calcium flux in the spinal cord.

Methods

Animals

Adult male Sprague–Dawley rats (200–250 g; SLAC Laboratory Animals; Shanghai, China) were bred in a room on a 12-h light/dark cycle and allowed free access to food and water. All surgical and experimental procedures were approved by the Animal Ethics Committee of Fudan University and followed the Guideline for Ethical Review of Animal Welfare (GB/T 35892-2018).

Surgery and behavioral tests

The rat model of NP was established using a previously reported method.[9] Briefly, animals were anesthetized using 1% sodium pentobarbital solution (40 mg/kg body weight). Rats were placed in the prone position, and the right forepaw was abducted and extended. A 1.5-cm-long horizontal incision was made in the skin 2 mm under the clavicle. Using micro-dissecting scissors, the pectoralis major muscle was exposed and cut parallel to the muscle fibers to expose the brachial plexus, leaving the cephalic vein intact. The subclavian vessels were located and protected. The upper, middle, and lower trunk were dissected, grasped with forceps, and extracted from the spinal cord by traction. The tissue layers were then brought together, and the skin was closed using 4–0 silk sutures. The brachial plexus was just dissected, but not avulsed, in the sham-operated group.

The mechanical withdrawal thresholds and cold allodynia were tested at five time points: day 0, and 1, 4, 7, and 10 days post-surgery. Mechanical allodynia was assessed using von Frey filaments (Stoelting, USA; bending force: 2.0, 4.0, 6.0, 8.0, 10.0, 15.0, and 26.0 g). Rats were placed in individual transparent plastic chambers (25×40×18 cm) with wire mesh bottoms and allowed to acclimatize to the environment for 30 mins. The filaments were applied to the middle surface of the left forepaw. The threshold was the lowest force that evoked a consistent and brisk withdrawal response. The bending force of the filament at which the rats responded in three out of five tests was defined as the withdrawal threshold.[9] Cold allodynia was measured using an acetone spray test. In this test, 250 μL of acetone was squirted onto the middle surface of the left forepaw. The withdrawal responses were evaluated on a scale of 0–3 points: (a) no response, 0 points, the paw was not moved; (b) mild response, 1 point, the paw had little or no weight on it; (c) moderate response, 2 points, the paw was elevated and was not in contact with any surface; and (d) robust response, 3 points, a vigorous response in which the rat licked, bit, or shook the paw.[9]

Animals exhibiting significant decreases in the pain threshold (mechanical threshold decreases from 15 g pre-surgery to 8 g post-surgery and allodynia score increases from 0 pre-surgery to 2–3 post-surgery) were placed in the NP group. Animals exhibiting no significant change in the pain threshold were assigned to the non-neuropathic pain (nNP) group. The sham-operated animals which brachial plexus was just dissected but not avulsed were assigned to the sham group. Animals without surgery were assigned to the blank group.

Immuno-fish

Rats were anesthetized using 1% pentobarbital and perfused transcardially with phosphate-buffered saline (PBS) and 4% paraformaldehyde. The C5-T1 segment of the spinal cord was harvested. The specimens were horizontally sectioned (10 μm) and mounted onto poly-l-lysine-coated slides. After desiccation for 20 mins at room temperature, the slides were rinsed twice for 5 mins with 1× saline-sodium citrate (SSC). The slides were then placed into a Coplin jar filled with antigen-unmasking buffer (10 mM sodium citrate). The Coplin

jar was placed into an autoclave, heated to 100°C for 5 mins, and then cooled to room temperature. The sections were washed 3 times for 5 mins with 1× SSC. To dehydrate the tissue sections, we immersed them for 3 mins each in a graded ethanol series (50%, 70%, 90%, and 100%). We then air-dried the sections for 10 mins. The pre-hybridization buffer (3% bovine serum albumin in 4× SSC) was warmed to approximately 47°C. Then, 200 μL of the warmed pre-hybridization buffer was pipetted onto each slide. The slides were pre-hybridized for 20 mins in a humid chamber. At the same time, the probes were diluted in hybridization buffer (1 g of dextran sulfate and 1 mL of deionized formamide in 9 mL of 4× SSC), denatured at 65°C for 10 mins, and then kept on ice. The pre-hybridization buffer was removed and 100 μL of the probe was added to each slide and hybridized overnight (4–16 hrs) at the same temperature used in the pre-hybridization step. From this step on, the slides were kept in the dark. After hybridization, the slides were rinsed with the following solutions: 4× SSC (for 5 mins, twice), 2× SSC (for 5 mins), 1× SSC (for 5 mins), and 0.1× SSC (for 5 mins) at the same temperature as that used in the hybridization step. Finally, the slides were rinsed with 1× PBS (for 5 mins) at room temperature. After in situ hybridization, the sections were incubated in blocking buffer (1 g of bovine serum albumin and 0.1 mL of Tween-20 in 100 mL of 1× PBS) for 30 mins at 37°C. After removing the blocking buffer, 200 μL of primary antibody diluted in blocking buffer was added to the sections. The sections were then incubated overnight at 4°C in a humid chamber and rinsed three times for 5 mins with 1× PBS. We then added the secondary antibody (200 μL diluted in blocking buffer) to the sections and incubated them for 2 hrs at 37°C. The slides were then rinsed three times for 5 mins with 1× PBS. Nuclear staining was performed using DAPI. Finally, 200 μL of antifade were added to the slides and the slides were coverslipped. We then sealed the coverslip onto the slide using nail polish. The antibodies and probes used in the test are listed in Tables S1 and S2.

Quantitative real-time PCR (qRT-PCR)

Rats were deeply anesthetized with pentobarbital and perfused transcardially with PBS. The C5–T1 section of the spinal cord was then immediately removed. The tissues were vertically separated, and hemisections of the spinal cord dorsal horn were subjected to total RNA extraction using mirVana™ miRNA Isolation Kit (cat. # AM1561; Ambion; Austin, TX, USA) according to the manufacturer's protocol. Total RNA was then purified using the RNeasy Mini Plus Kit (Qiagen, USA). The amount of total RNA was quantified using a Nanodrop spectrophotometer (Nanodrop ND2000, Thermo Fisher). Reverse transcription was performed on 100 ng of total RNA using PrimeScript RT Reagent Kit with gDNA Eraser (cat. # RR047A, Takara, Japan). Quantitative PCR was performed using SYBR Premix Ex Taq II (cat. # RR820A, Takara, Japan) and a LightCycler 96 (Roche, Switzerland). Expression levels were normalized to the values for GAPDH. The full sequence of rat Malat1 was obtained from NCBI (Figure S1). Three pairs of primers were designed and synthesized for Malat1 to ensure the reliability of outcomes.

Primary neuron culture

Primary cultures of cortical neurons were prepared from E16 Sprague–Dawley rats, as previously described.[10] Pregnant rats were anesthetized. After preparing the skin for surgery, the fetuses were harvested into a sterile petri dish containing cold HBSS. The skull, cerebral dura mater, and pia mater were removed under a microscope (Zeiss, Germany). A piece of cortex was harvested and placed into a sterile 35 mm petri dish containing cold HG-DMEM. The tissue was cut into small pieces approximately 1 mm in length. Then, 1 mL of papain (2 mg/mL dissolved in HG-DMEM) was added to the petri dish, and the tissue was digested for 30 mins in a 37°C incubator. DNase I (200 μL, 2.5 mg/mL dissolved in HG-DMEM) was then added to the tissue for 30 s. Finally, 1 mL of HG-DMEM containing 10% FBS was added to the tissue terminate the digestion. The contents of the petri dish were transferred to a 15-mL sterile centrifuge tube and triturated gently 20 times using a Pasteur pipette. After allowing the tissue to settle for 2 mins, 1 mL of the supernatant was collected into another 15-mL sterile centrifuge tube. One milliliter of HG-DMEM containing 10% FBS was then added to the former centrifuge tube. The triturating, settling, and collecting steps were repeated 3 more times to yield 4 mL of the cell suspension. The cell suspension was filtered twice through a sieve with a pore diameter of 70 μm. The filtrate was centrifuged at 800 rpm for 5 mins, and the supernatant was removed. HG-DMEM containing 10% FBS was used to resuspend the cells. The density of the cell suspension was adjusted to 100,000 cells per milliliter. The cells were seeded onto PDL (molecular weight: 70,000–150,000, cat. # P6407, Sigma) and laminin (cat. # 23017–015, Gibco) double-coated 6-well culture plates at a density of 50,000 cells per cm^2 and cultured in a 37°C incubator in an atmosphere of 5% carbon dioxide. After 4 hrs of incubation, the media was

changed to Neurobasal medium (cat. # 21103049, Gibco) containing 2% B27 supplement, 1% penicillin-streptomycin, and 1% Glutamax (cat. # 35050061, Gibco). The media was refreshed by exchanging half of the volume with fresh media every two days.

Synthesis of adenovirus vectors for Malat1 interference

Full-length Malat1 cDNA and three full-length Malat1 antisense cDNAs were synthesized and identified by clone sequencing. Restriction enzyme (EcoRI/BamHI) recognition sites were introduced at the 5′ and 3′ ends of the four fragments. The identified fragments were ligated into the EcoRI/BamHI sites of the proviral plasmids (pHBAd-EF1-MCS-GFP, Hanbio Biotechnology, China). Adenovirus vectors were generated by triple transfection of HEK293 cells. Viral lysate was harvested 12 days post-transfection using freeze-thaw cycles. The viral lysate was purified using a combination of CsCl density gradient centrifugation and dialysis. The vectors were stored in aliquots at −80°C until use. The sequences of the primers and transcripts are shown in Tables S3 and S4. The validation of RNA interference is shown in Figure S3.

Apoptosis test

Neuronal apoptosis after Malat1 interference was assessed using the In Situ Cell Death Detection Kit (cat. # 11684817910, Roche, Switzerland). We performed the Malat1 interference experiment in primary cortical neurons on the fourth day of culture using virus vectors. The cells were fixed and stained on the seventh day of culture. Staining was performed according to the manufacturer's instructions. Positive control and negative control group were made following the manufacturer's instruction. Neurons with upregulated Malat1 were labeled as up group. Neurons with downregulated Malat1 were labeled as down group. Neurons without Malat1 interference were labeled as blank group. The positive cells were counted under a microscope. The proportions of positive cells were statistically analyzed.

Calcium imaging and quantification

On the 14th day of primary neuron culture, media were removed and neurons were immersed in HBSS for 3 times. Then, the neurons were incubated with the calcium indicator Fura-2 AM (5 μL/mL dissolved in HBSS, cat. # F1225, Thermo Fisher) for 60 mins at 37°C. The neurons were then immersed in HBSS (cat. # 14170112, Gibco) 3 times and incubated in HBSS (containing 0.22 mg/mL $CaCl_2$) for 30 mins at 37°C. A laser confocal fluorescence microscope (Olympus FluoView FV1000) equipped with a drug perfusion system was used for recording and analysis of the results.

Fluorescence images of a fixed frame were acquired using a digital camera every 2 s. Fluorescence intensity changes in response to 340 nm and 380 nm excitation were recorded. Glutamic acid (1 mmol/L diluted in HBSS) was used to stimulate the neurons for 1 min and was then removed. The ratio of fluorescence intensity under excitation at 340 nm to that under excitation at 380 nm was defined as the R score. We obtained R score curves for each series of fluorescence images. The amplitude of the curve was used to quantify the increase in calcium in neurons under stimulation from glutamic acid. Differences between groups were analyzed using Mann–Whitney U tests.

MEA experiments

Primary cortical neurons of fetal rats were collected as part 2.5. Neurons were plated at a density of 5×10^5 cells/mL (high density) in a volume of 500 μL on PDL/laminin-coated 60-microelectrode dishes (60MEA200/30iR-Ti, Multi Channel Systems MCS GmbH, Germany). The dishes had 60 microelectrodes at the bottom. Electrical activity of neurons could be detected by these microelectrodes and recorded by an external MEA system. Neurons were cultured in a 37°C incubator in an atmosphere of 5% carbon dioxide. The culture media was same with part 2.5 and replenished in a 1:3 ratio every 2 days. On the 4th day, adenovirus vectors used to regulate Malat1 expression were transferred to the cultures at an MOI of 100, as indicated in the manufacturer instructions. The cell culture plates were categorized as upregulated, downregulated, control, or blank group based on the vector used. Recordings of neurons spontaneous spike from each array were obtained every week using the MEA system (MEA2100, Multi Channel Systems MCS GmbH). To obtain extracellular recordings, the multi-electrode arrays were placed into the recording chambers and maintained at 37°C. Baseline recordings were performed for 2 mins prior to acquiring 2-min recordings. We analyzed spontaneous spikes using MC_RACK software (Multi Channel Systems) with a filter threshold set to 120 mV. The frequency of spontaneous spikes of each group was statistically analyzed.

Statistics

Statistical significance was determined using paired Student's t-tests (Figures 1A and 2), Wilcoxon signed-rank tests (Figure 1B), unpaired Student's t-tests (Figures 4 and 5C) or

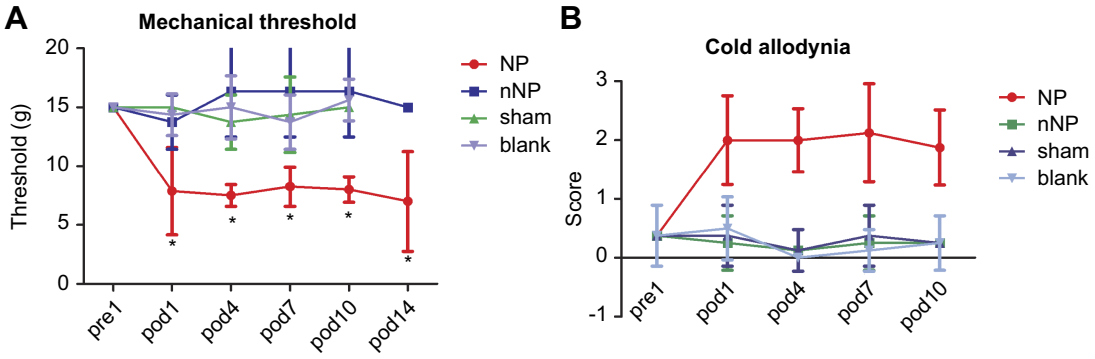

Figure 1 Mechanical and cold pain thresholds measurement. (**A**) Change of mechanical threshold tested by von Frey (n=8, *p<0.05, paired Student's t-test). (**B**) Change of cold allodynia tested by squirting acetone onto the middle surface of the left forepaw (n=8, *p<0.05, Wilcoxon signed-rank test).

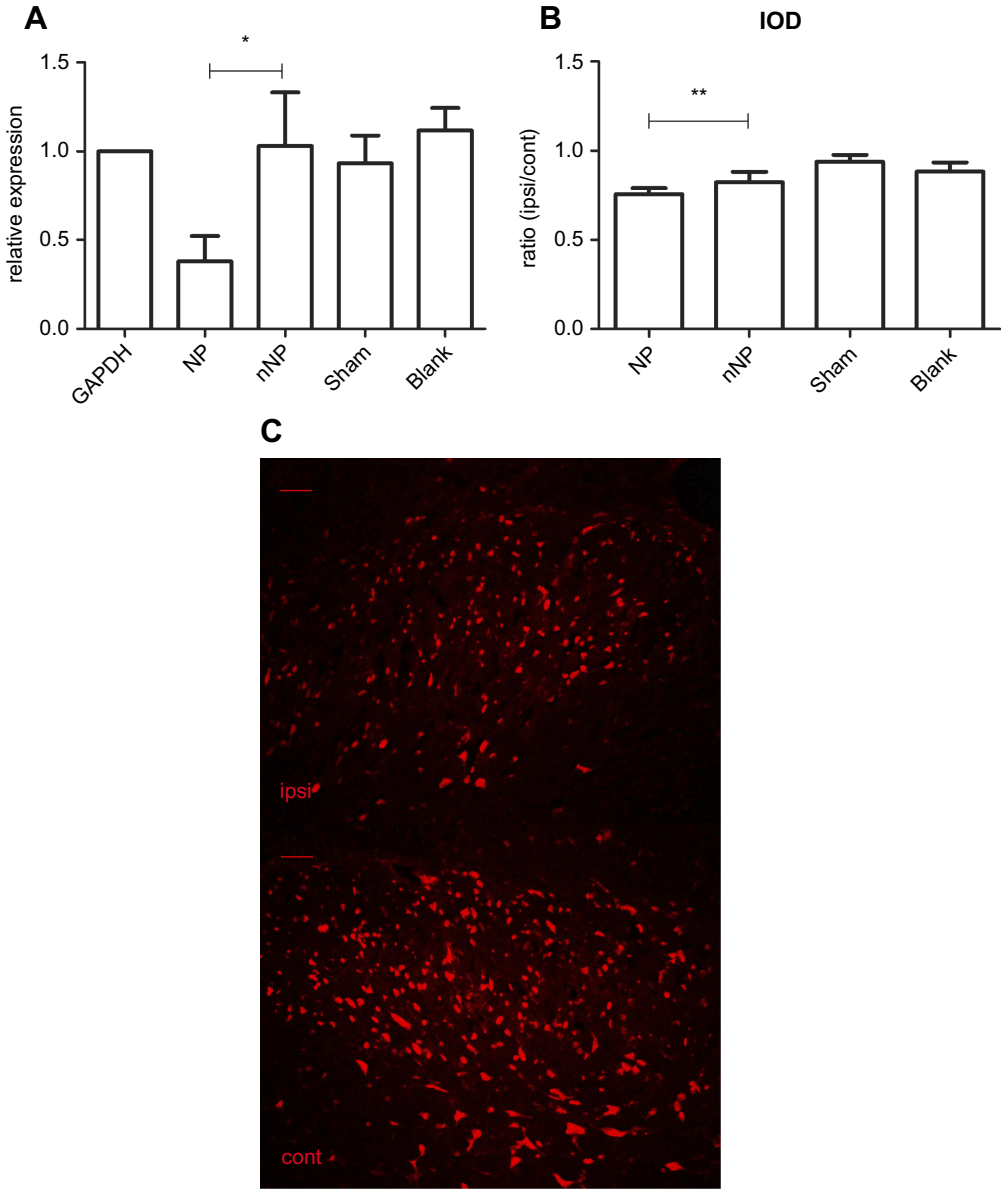

Figure 2 Quantitative test of malat1 expression. (A) Quantitative real-time PCR analysis of malat1 expression in spinal cord dorsal horn after brachial plexus avulsion, with GAPDH serving as reference gene (n=6; *p<0.01, paired Student's t-test). (**B**) Quantitative analysis of IOD ratio of ipsilateral to contralateral spinal cord dorsal horn between rats in the NP and nNP groups (n=6, **p<0.05, paired Student's t-test). (**C**) Fluorescence in situ hybridization of ipsilateral and contralateral spinal cord dorsal horn from NP rat (scale bar=200 μm).

Mann–Whitney U tests (Figure 6) in SPSS 20.0 software. Differences with p values <0.05 were considered significant.

Results

Mechanical and cold pain thresholds were decreased in NP rats

The mechanical and cold pain thresholds were determined based on the withdrawal responses of the rat's left forepaw to mechanical and cold stimulation delivered using von-Frey filaments and acetone, respectively. To compare changes in the mechanical pain threshold, we used animals that had a pre-operation mechanical pain threshold of 15 g. After brachial plexus avulsion, the mechanical pain threshold decreased to about 8 g on the first day post-operation in the NP group. This decrease in the pain threshold lasted for at least 10 days (Figure 1A). The cold pain score was 0 in all groups pre-operation, but increased to 2 or higher in the NP group. This increase was also observed on the first day post-operation and lasted for at least 10 days (Figure 1B). These data indicate that both the mechanical pain threshold and the cold pain threshold were decreased in the NP group when compared to those in the control group. This reflected a state of hyperalgesia and cold allodynia in the animals in the NP group.

The levels of lncRNA Malat1 were decreased in the spinal cord in the NP rats

The qRT-PCR experiments revealed significantly decreased Malat1 levels in the NP when compared to the nNP group (p<0.01, Figure 2A). There was no significant difference in Malat1 levels between the nNP and sham groups. The qRT-PCR results were consistent with those of our previous experiments using microarrays. We also quantified Malat1 expression based on the integrated optical density (IOD) in the spinal cord dorsal horn and compared the ipsilateral to contralateral IOD ratio between rats in the NP and nNP groups. Our data indicated that the IOD ratio was significantly lower in the NP group than in the nNP group. This further confirmed the decrease in Malat1 levels in the spinal cords of NP rats (Figure 2B and C). Taken together, these data indicate that Malat1 is a potential regulator of NP.

LncRNA Malat1 was expressed in neurons

To investigate the spatial distribution of Malat1 expression in the spinal cord, we performed immuno-FISH on frozen spinal cord sections from rats. Three oligonucleotide probes were designed. NeuN, GFAP, and Iba-1 were used as markers of neurons, astrocytes, and microglia, respectively. All Malat1-positive cells in the spinal cord were also positive for NeuN, but not for GFAP or Iba-1. This showed that Malat1 was expressed in neurons, but not astrocytes or microglia (Figure 3).

The downregulation of malat1 did not affect neuronal apoptosis

We cultured primary neurons from fetal rats. On the 7th day after plating, we performed Nissl staining and immunofluorescence experiments to assess the purity of the neuronal culture. Most of the cells were MAP-2-positive (Figure S2). We asked whether the dysregulation of Malat1 mediated by the adenovirus vectors affected neuronal apoptosis. After transfecting the cells with the virus, neuronal apoptosis was assessed using TUNEL. When compared to the positive control (Figure 4A), cells with upregulated Malat1 expression (Figure 4C), those with downregulated Malat1 expression (Figure 4D), and untreated cells (Figure 4E) had a very low ratio of TUNEL-positive cells to total cells, similar to cells treated with the negative control (Figure 4B). There was no significant difference between cells with upregulated Malat1 expression and those with downregulated Malat1 expression (Figure 4F). These results indicate that the dysregulation of Malat1 had no effect on neuronal apoptosis.

Decreased Malat1 expression resulted in increased spontaneous electrical activity in neurons

Neurons grown on MEA dishes displayed good coverage over all microelectrodes (Figure 5A). Typical neuronal growth and electrical activity were observed in dishes without virus transfer (Figure 5B). No spontaneous spikes were observed in any of the plates on the 7th day after plating. On the 14th day after plating, obvious spontaneous spike trains were recorded in all plates. The spontaneous spike trains were still present on the 21st day after plating. Differences in spontaneous spike frequency on the 14th day after plating between different groups were statistically analyzed using Student's t-tests. The spontaneous spike frequency was significantly higher in the Malat1 downregulated group than in the Malat1 upregulated group (p<0.0001). There was no significant difference between the Malat1 upregulated group and the control group (p=0.9271, Figure 5C).

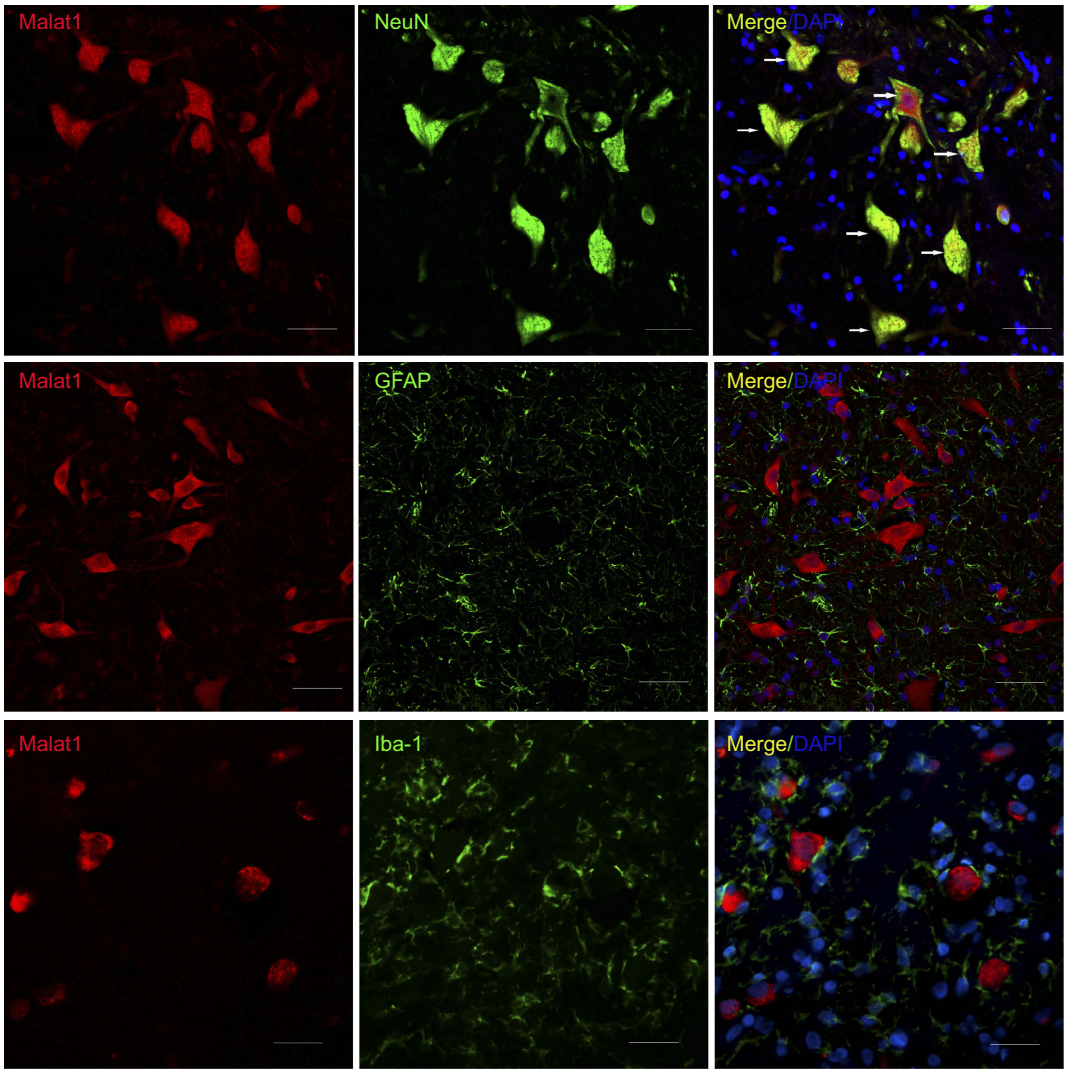

Figure 3 The spatial distribution of malat1 in rats' spinal cord. The biomarker of neurons (NeuN, top panel), astrocytes (GFAP, middle panel) and microglia (Iba-1, bottom panel) are labeled with green fluorescence. Malat1 is labeled with red fluorescence. Nuclear is labeled with blue fluorescence. Only NeuN-positive cells are double labeled (white arrow). Scale bars =50 μm.

Reactivity of Malat1 downregulated neurons to glutamic acid stimulation

The reactivity of neurons to glutamic acid stimulation was assessed using calcium imaging. Glutamic acid binds receptors on neurons and leads to an influx of calcium. This in turn leads to an increase in the number of Fura-2-calcium complexes in neurons, resulting in increased fluorescence intensity under excitation at 340 nm. The R score, which is defined as the ratio of fluorescence intensity under excitation at 340 nm to that under excitation at 380 nm, was used to quantify the reactivity of neurons to glutamic acid stimulation. Figure 6A shows the R score curve for normal neurons. The amplitudes of the R score curves for neurons with altered Malat1 expression were statistically analyzed using Mann–Whitney U tests. The amplitude of the R score curve for the Malat1 downregulated group was significantly higher than that for the blank group (Figure 6B, p=0.05, n=3). There was no significant difference between the Malat1 downregulated and Malat1 upregulated groups (Figure 6B, p=0.20, n=3).

Discussion

The mammalian genome contains thousands of lncRNAs.[6] LncRNAs have recently gained widespread attention due to their potential roles in many biological processes and disorders.[11] Malat1 is a widely expressed and evolutionarily conserved lncRNA, which was originally found in lung cancer cells. Its expression is related to metastasis and invasiveness of cancer.[12] In this study, we investigated the expression of Malat1 in the spinal cord of brachial plexus avulsion-induced NP rats and the potential mechanisms by

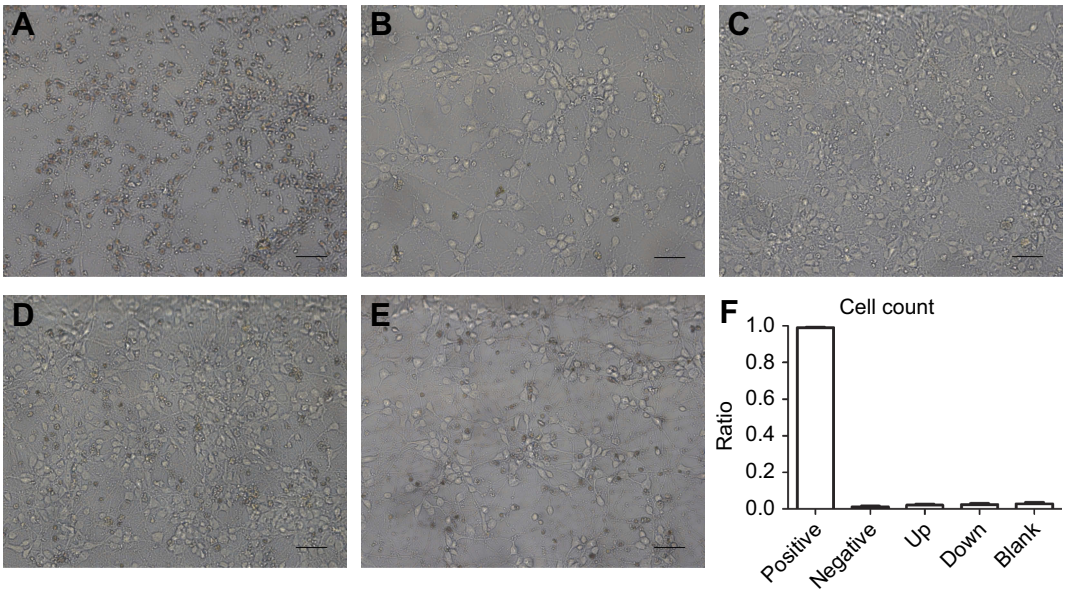

Figure 4 Neurons apoptosis after malat1 dysregulation tested by TUNEL. (**A**) Positive control. (**B**) Negative control. (**C**) Malat1 upregulated group. (**D**) Malat1 downregulated group. (**E**) Blank group. (**F**) Comparison of the ratio of neurons apoptosis in each group. Neuron apoptosis is labeled as brown. The difference between upregulated and downregulated group is not significant (n=6, Students' *t* test). Scale bar=200 μm.

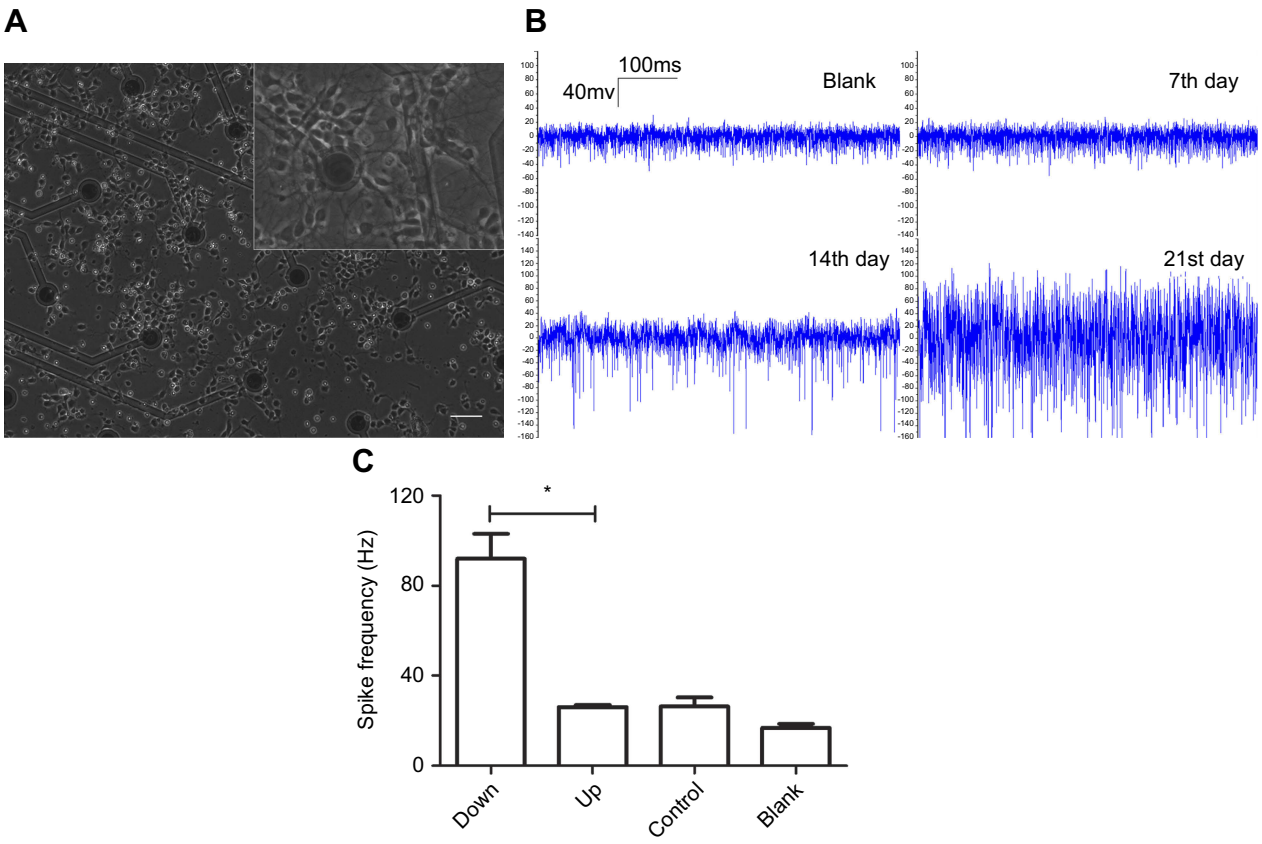

Figure 5 MEA analysis of spontaneous electricity of neurons. (A) Neurons growth on MEA electrode. Scale bar =200 μm. (**B**) Spontaneous electricity of normal neurons recording on the 7th, 14th, 21st day of culture with blank array as negative control. (**C**) Comparison of spontaneous spike frequency recording at the 14th day. Neurons with downregulated Malat1 are labeled as down group. Neurons with upregulated Malat1 are labeled as up group. Normal neurons are in control group. Blank group has no neurons. The spike frequency is significantly different between malat1 downregulated and upregulated group (*p<0.0001, Students' *t* test).

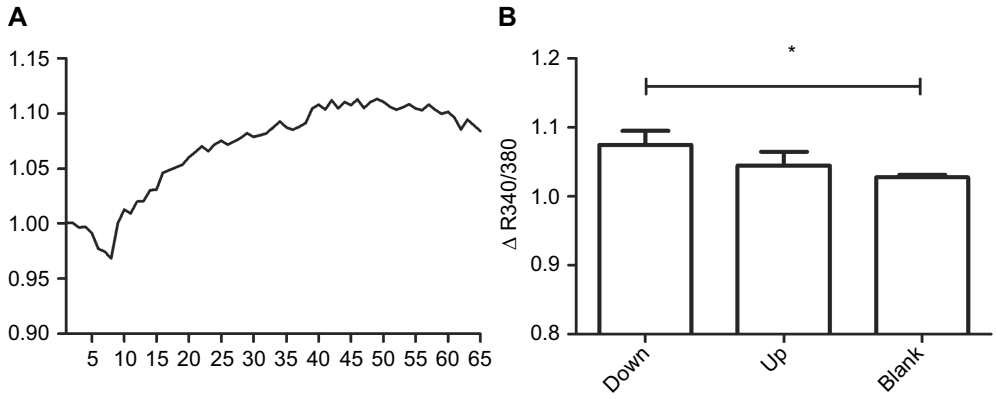

Figure 6 Reactivity of neurons to the stimulation of glutamic acid analyzed via calcium imaging method. R score is the ratio of fluorescence intensity under excitation at 340 nm and 380 nm. (**A**) The curve of R score of normal neurons under the stimulation of glutamic acid. (**B**) Comparison of the amplitude of R score curve of each group. Malat1 is upregulated in up group and downregulated in down group. Blank group has normal neurons. Neurons in the Malat1 downregulated group has significantly higher reactivity than that in the blank group (*p=0.05, n=3, Mann–Whitney U test).

which Malat1 may regulate NP. We found that Malat1 had decreased expression in the spinal cord in NP rats after brachial plexus avulsion. Further in vitro studies revealed that the decreased expression of Malat1 might result in NP by increasing the excitability of neurons, potentially by regulating the transmembrane flow of calcium ions.

In our study, we found that lncRNA Malat1 was expressed in neurons in the spinal cord dorsal horn, but not in microglia or astrocytes. Malat1 was downregulated in the spinal cord in NP rats after brachial plexus avulsion. We downregulated the expression of Malat1 in vitro using adenovirus vectors and found that Malat1 downregulation increased the frequency of spontaneous electrical activity in neurons. Malat1 upregulation had no significant effect on neuronal electrical activity. These findings indicated that reduced Malat1 expression may lead to increased excitability of neurons. Current understanding of the pathogenesis of NP is mainly focused on peripheral and central sensitization.[13] Despite increasing evidence highlighting the importance of peripheral sensitization, many investigators believe that changes in the spinal cord and brain, such as increased excitability of neurons, and neuron-glial cell interactions are the main internal processes underlying NP.[4,14] Regardless of whether the cause of pain is peripheral or central origin, development and maintenance of NP is ultimately associated with increased electrical activity in sensory conduction neurons or decreased electrical activity in inhibitory interneurons. Primary sensory neurons in the dorsal root ganglion (DRG) and secondary sensory neurons in the spinal cord dorsal horn are important parts of the pain transmission pathway and have important roles in the modulation of pain.[15] It has been reported that the expression of TNF-α and IL-1β and their receptors is increased in the DRG in rats after peripheral nerve injury.[16,17] Exogenous injections of TNF-α and IL-1β into the DRG in healthy rats can induce hyperalgesia.[18] TNF-α may lead to NP by activating multiple signaling pathways in neurons which can increase the expression of ion channel and result in increased electrical activity. It has been reported that TNF-α can act on its receptor on neurons and activate the p38-MAPK signaling pathway. This would lead to increased activation of tetrodotoxin-resistant sodium ion channels, which in turn would sensitize DRG neurons to mechanical stimulation.[19] TNF-α can also promote the expression of transient receptor potential vanilloid-1 (TRPV1) on the surface of DRG neurons via the ERK-MAPK signaling pathway.[20] TRPV1 is a sensor for noxious heat and plays an important role in the pathogenesis of heat hyperalgesia.[21] In the spinal cord of animal models of NP, the electrical activity of sensory neurons is altered after peripheral nerve injury. Researchers have found that Aβ nerve fibers, which do not initially induce pain stimulation, were phenotypically transformed and had increased secretion of substance p and calcitonin gene-related peptide (CGRP) in animal models of NP.[22,23] Substance p binds to its receptor, NK1, on the postsynaptic membrane and leads to sustained depolarization of neurons. CGRP not only enhances the effects of substance p but also binds to its receptors to activate protein kinases PKA and PKC, which phosphorylate glutamate receptors on neurons. This, in turn, leads to increased reactivity of neurons to glutamate, which is the main excitatory transmitter.[24] Both substance p and CGRP can thus increase the electrical activity of sensory neurons.

We explored potential mechanisms underlying the increased electrical activity of neurons following Malat1 downregulation using calcium imaging. In the presence of glutamate stimulation, there were greater changes in intracellular calcium concentration in Malat1 downregulated neurons than in control-treated neurons. We, therefore, speculated that Malat1 downregulation led to increased electrical activity in neurons by activating calcium-related channels. The specific mechanism by which Malat1 regulates calcium transmembrane flow has not yet been reported. However, some non-selective cation channels also allow the passage of calcium ions. The glutamate receptor NMDA is a non-selective cation channel that, upon activation, allows calcium ions to flow across the membrane. This, in turn, leads to an increase in intracellular calcium concentration. There is a complex interaction between NMDA activation and the MAPK signaling pathway.[25] Normally, glutamate binding to NMDA can activate the MAPK signaling pathway.[26] It has been reported that reduced Malat1 expression in glioma cells and retinal endothelial cells can also activate the MAPK signaling pathway.[27,28] These results suggest that Malat1-induced changes in intracellular calcium concentration might result from NMDA receptor activity and downstream activation of the MAPK signaling pathway. However, further studies are still necessary to explore the mechanisms.

The gate control theory of pain modulation suggests that the inhibitory interneurons in the spinal cord dorsal horn are excited by peripherally afferent fibers and can secrete inhibitory neurotransmitters that reduce the electrical activity of sensory neurons and inhibit the conduction of pain signals.[29] It has been reported that these inhibitory interneurons undergo apoptosis after peripheral nerve injury. This leads to reduced inhibition of pain signal conduction, which is a pathogenic mechanism underlying NP. A variety of animal models of NP display neuronal apoptosis in the spinal cord, especially in neurons in lamina II of the spinal cord dorsal horn,[30] which contains the inhibitory interneurons.[31] A study on liver cancer revealed that decreased Malat1 expression led to increased cancer cell apoptosis.[32] However, in our study, we altered Malat1 expression in cultured neurons in vitro. TUNEL staining revealed no significant apoptosis of neurons in both the Malat1 upregulated and downregulated groups. This indicates that reduced expression of Malat1 does not induce NP by affecting neuronal apoptosis. This is consistent with previous studies reporting that Malat1 was not indispensable for cell survival and development.[33,34]

In conclusion, we investigated the expression levels and the role of lncRNA Malat1 in the regulation of NP in brachial plexus avulsion rats. Malat1 was identified in the cytoplasm in neurons, and its expression level decreased in the spinal cord in NP rats after brachial plexus avulsion. Reduced Malat1 expression may contribute to neuropathic pain by increasing neuronal excitability via regulation of calcium flux without affecting neuronal survival. This study thus provides new insight into the pathogenesis of NP and may lead to a novel therapeutic strategy for the treatment of this condition.

Acknowledgments

This work was supported by the Ministry of Science and Technology of China (973 Program Grant 2014CB542204 to Yun Wang), National Natural Science Foundation of China (NSFC 81572127 to Jie Lao), National Natural Science Foundation of China (NSFC 81501051 to Jing Rui) and Sanming Project of Medicine in Shenzhen (grant number SZSM201512032).

Disclosure

The authors report no conflicts of interest in this work.

References

1. Geber C, Baumgärtner U, Schwab R, et al. Revised definition of neuropathic pain and its grading system: an open case series illustrating its use in clinical practice. *Am J Med*. 2009;122(10 Suppl):S3–S12. doi:10.1016/j.amjmed.2009.04.005
2. Tantigate D, Wongtrakul S, Vathana T, Limthongthang R, Songcharoen P. Neuropathic pain in brachial plexus injury. *Hand Surg*. 2015;20(1):39–45. doi:10.1142/S0218810415500057
3. Teixeira MJ, Da Paz MGDS, Bina MT, et al. Neuropathic pain after brachial plexus avulsion–central and peripheral mechanisms. *BMC Neurol*. 2015;15:73. doi:10.1186/s12883-015-0329-x
4. Kuner R. Central mechanisms of pathological pain. *Nat Med*. 2010;16(11):1258–1266. doi:10.1038/nm.2231
5. Qureshi IA, Mattick JS, Mehler MF. Long non-coding RNAs in nervous system function and disease. *Brain Res*. 2010;1338:20–35. doi:10.1016/j.brainres.2010.03.110
6. Lee JT. Epigenetic regulation by long noncoding RNAs. *Science*. 2012;338(6113):1435–1439. doi:10.1126/science.1231776
7. Zhao X, Tang Z, Zhang H, et al. A long noncoding RNA contributes to neuropathic pain by silencing Kcna2 in primary afferent neurons. *Nat Neurosci*. 2013;16(8):1024–1031. doi:10.1038/nn.3438
8. Sandkuhler J. Models and mechanisms of hyperalgesia and allodynia. *Physiol Rev*. 2009;89(2):707–758. doi:10.1152/physrev.00025.2008
9. Wang L, Yuzhou L, Yingjie Z, Jie L, Xin Z. A new rat model of neuropathic pain: complete brachial plexus avulsion. *Neurosci Lett*. 2015;589:52–56. doi:10.1016/j.neulet.2015.01.033
10. Xu SY, Wu Y-M, Ji Z, Gao X-Y, Pan S-Y. A modified technique for culturing primary fetal rat cortical neurons. *J Biomed Biotechnol*. 2012;2012:803930. doi:10.1155/2012/803930
11. Ponting CP, Oliver PL, Reik W. Evolution and functions of long noncoding RNAs. *Cell*. 2009;136(4):629–641. doi:10.1016/j.cell.2009.02.006
12. Ji P, Diederichs S, Wang W, et al. MALAT-1, a novel noncoding RNA, and thymosin beta4 predict metastasis and survival in early-stage non-small cell lung cancer. *Oncogene*. 2003;22(39):8031–8041. doi:10.1038/sj.onc.1206928

13. Baron R, Binder A, Wasner G. Neuropathic pain: diagnosis, pathophysiological mechanisms, and treatment. *Lancet Neurol*. 2010;9(8):807–819. doi:10.1016/S1474-4422(10)70143-5
14. Latremoliere A, Woolf CJ. Central sensitization: a generator of pain hypersensitivity by central neural plasticity. *J Pain*. 2009;10(9):895–926. doi:10.1016/j.jpain.2009.06.012
15. Bourne S, Machado AG, Nagel SJ. Basic anatomy and physiology of pain pathways. *Neurosurg Clin N Am*. 2014;25(4):629–638. doi:10.1016/j.nec.2014.06.001
16. Schäfers M, Sommer C, Geis C, Hagenacker T, Vandenabeele P, Sorkin LS. Selective stimulation of either tumor necrosis factor receptor differentially induces pain behavior in vivo and ectopic activity in sensory neurons in vitro. *Neuroscience*. 2008;157(2):414–423. doi:10.1016/j.neuroscience.2008.08.067
17. Opree A, Kress M. Involvement of the proinflammatory cytokines tumor necrosis factor-alpha, IL-1 beta, and IL-6 but not IL-8 in the development of heat hyperalgesia: effects on heat-evoked calcitonin gene-related peptide release from rat skin. *J Neurosci*. 2000;20(16):6289–6293.
18. Schäfers M, Lee DH, Brors D, Yaksh TL, Sorkin LS. Increased sensitivity of injured and adjacent uninjured rat primary sensory neurons to exogenous tumor necrosis factor-alpha after spinal nerve ligation. *J Neurosci*. 2003;23(7):3028–3038.
19. Jin X, Gereau RWT. Acute p38-mediated modulation of tetrodotoxin-resistant sodium channels in mouse sensory neurons by tumor necrosis factor-alpha. *J Neurosci*. 2006;26(1):246–255. doi:10.1523/JNEUROSCI.3858-05.2006
20. Hensellek S, Brell P, Schaible H-G, Bräuer R, Segond von Banchet G. The cytokine TNFalpha increases the proportion of DRG neurones expressing the TRPV1 receptor via the TNFR1 receptor and ERK activation. *Mol Cell Neurosci*. 2007;36(3):381–391. doi:10.1016/j.mcn.2007.07.010
21. Kim YS, Chu Y, Han L, et al. Central terminal sensitization of TRPV1 by descending serotonergic facilitation modulates chronic pain. *Neuron*. 2014;81(4):873–887. doi:10.1016/j.neuron.2013.12.011
22. Nitzan-Luques A, Minert A, Devor M, Tal M. Dynamic genotype-selective "phenotypic switching" of CGRP expression contributes to differential neuropathic pain phenotype. *Experimental Neurology*. 2013;250:194–204. doi:10.1016/j.expneurol.2013.09.011
23. Nitzan-Luques A, Devor M, Tal M. Genotype-selective phenotypic switch in primary afferent neurons contributes to neuropathic pain. *Pain*. 2011;152(10):2413–2426. doi:10.1016/j.pain.2011.07.012
24. Aira Z, Buesa I, García Del Caño G, et al. Transient, 5-HT2B receptor-mediated facilitation in neuropathic pain: up-regulation of PKCγ and engagement of the NMDA receptor in dorsal horn neurons. *Pain*. 2013;154(9):1865–1877. doi:10.1016/j.pain.2013.06.009
25. Haddad JJ. N-methyl-D-aspartate (NMDA) and the regulation of mitogen-activated protein kinase (MAPK) signaling pathways: a revolving neurochemical axis for therapeutic intervention? *Prog Neurobiol*. 2005;77(4):252–282. doi:10.1016/j.pneurobio.2005.10.008
26. Fan J, Gladding CM, Wang L, et al. P38 MAPK is involved in enhanced NMDA receptor-dependent excitotoxicity in YAC transgenic mouse model of Huntington disease. *Neurobiol Dis*. 2012;45(3):999–1009. doi:10.1016/j.nbd.2011.12.019
27. Liu J-Y, Yao J, Li X-M, et al. Pathogenic role of lncRNA-MALAT1 in endothelial cell dysfunction in diabetes mellitus. *Cell Death Dis*. 2014;5:e1506. doi:10.1038/cddis.2014.466
28. Han Y, Wu Z, Wu T, et al. Tumor-suppressive function of long noncoding RNA MALAT1 in glioma cells by downregulation of MMP2 and inactivation of ERK/MAPK signaling. *Cell Death Dis*. 2016;7:e2123. doi:10.1038/cddis.2015.407
29. Melzack R, Wall PD. Pain mechanisms: a new theory. *Science*. 1965;150(3699):971–979.
30. Scholz J, Broom DC, Youn D-H, et al. Blocking caspase activity prevents transsynaptic neuronal apoptosis and the loss of inhibition in lamina II of the dorsal horn after peripheral nerve injury. *J Neurosci*. 2005;25(32):7317–7323. doi:10.1523/JNEUROSCI.1526-05.2005
31. Todd AJ. Neuronal circuitry for pain processing in the dorsal horn. *Nat Rev Neurosci*. 2010;11(12):823–836. doi:10.1038/nrn2947
32. Lai M-C, Yang Z, Zhou L, et al. Long non-coding RNA MALAT-1 overexpression predicts tumor recurrence of hepatocellular carcinoma after liver transplantation. *Med Oncol*. 2012;29(3):1810–1816. doi:10.1007/s12032-011-0004-z
33. Eissmann M, Gutschner T, Hämmerle M, et al. Loss of the abundant nuclear non-coding RNA MALAT1 is compatible with life and development. *Rna Biology*. 2012;9(8):1076–1087. doi:10.4161/rna.21089
34. Zhang B, Arun G, Mao YS, et al. The lncRNA Malat1 is dispensable for mouse development but its transcription plays a cis-regulatory role in the adult. *Cell Reports*. 2012;2(1):111–123. doi:10.1016/j.celrep.2012.06.003

Supplementary materials

5′-
tgcgtcaggcattcaggcagcgagcacaggcacctggtgaggcaggagactcagcctgaggcattcgcagataagtttctattt
aaaaagatttaaaaggaaactagaactctaaacttaatagagtagcttactgagataataatattttaatattaagattttaaaa
gaaaagtatggaggtttatttaaacaatttgaaaaaggaaaagagaaaaatttttgtaccaccagatggaggctgacctgagg
cgtttattcagagtagtttagaagattgtaaaagggagcaattgtggagtttcaaaggttctagcttgagggtcagccttgttagg
tgtacttttaaacgaaggttacctaaacagaatctaaatggctttttaaaattgtaaagttgtagataatagtttgaaaatgagat
gtagtttaaaaagattgaaaaaagtaagttgaagggcgttataagagtcgactgtcgcatgtacgaaggcatgagttggaaac
ggggaatggaagtggtagggttagtattttgagaaagaagattagaaaatggaagtggaaaaatgaagacaagttcaggaag
gtgaagaaaagctgtagagaagataggaaaatagaagaccgaagaatcattagaagacagaaaaggtatttaaacacacag
gtaggaagaaaactagaagatagaaaaaaagcaagatagaaagacaaaaggaagttcagacaactttggatgccagcattc
aagataggcaaagaagataagatcaagaccaaaaggttggataaggttaaatctcagaaataaagtcagaaggaaattattt
ttaaagccataaattcaagtttctgatggagcccagcagtttagaagtgtctgtagacagccattttacaagagtgaagctagca
gtcaaagctacaactgaagtaattaaaaaggcagaatgcgtttgaaaagttagaagaatattagaagccttaacttgtagctta
attttgttttgagaacaaaaggacttttgataacaatttcaagattgtcagcattttgcattggacttgagctgaggtgctttaaaa
gtgttaacgactagcattggcagccgaccaaggtctacacagaagtggattcagtgaacctaggaagacaggagtcccgaagc
cagtttggtgaagctaggaaggactgagcagccagcagcagcaggtcatggtgaagatagcccaggaaacagtgcggttcgtt
ggaggaagctaggaagaaggagccgaaatgatgtggtgaagctagaaaagaggattccgggaaggtggagccagttcgagt
tggtgatgaagctagctggcgtcttggcttgtcaacgcggaggaggcgagcaggcattgcgttgtggagagaatagatagcgg
ctcctagaccagcatgtcaatgtgcaagaaaggctgcagggaaagcatgtggtgcggtaacatcccgtgaggtcggcaacgcg
gtggtggtttctgtaacttgaggatggtaacttgtttattttgccttggtatgggggagtttgtaggcttctgtctgtatccactggtg
ctgccaaggctgtggacaaggtcatcccagaagagagtcatctggggctgtaggccgctgcgggtgttggaggtttttctttttca
gggttgtgtcctcttgcatcttgtctgaagcttttgagggcagactgccaaggcccagaagaatggtagatggcaagttgtcttaa
cccgatctgagggaaaatgaatggtagagccaacagtctcgccagttttgtaagacgttttagttctgtgaacagctaacctact
gcagtcttctgcaagtcttactactgtgtaggggaggtaattgggcaaagtgcttgggggtggggtgggacaaaatatattttg
agttcttttcccctaggtctgtctagaatcctaaaggcagatgactcaagggaaccaggaaaaaaagaaaatccagtatcagg
ataagcagaactcaacaggtttacagtttctagaaattagatgaatagctttcacgttgaatatggaggagctgtccattggcga
aatggctggtagtttattcttttccccctcccttaacaagacttgtaaaattcctaatcttttgaatatttttacttgaaatatttggga
atggtcttaacagggaggagtgggtgggggaaaatgtttttttctaagattttccacagatgctatagttctgttggcacactgggt
tagagaaggcgtgtactgctatgctgttggcacgacaccttcagggactggagctgccctttatccttggaagagtttccccagtg
gccgctgaagtacagcacagtgcagctttggttcacagtcacctcaggagaacctcaggagcttgagtaggccagatgttaaag
ttaagttttcaagcaccatgacnnnnnnnnnnnnnnnnnnnnnnnnnnnnnnnnnnnnnnnnnnnnnnnnnnnnnnnnnnnnn
nnnnnnnnnnnnnnnnnn-3′

Figure S1 The full-length rat Malat1 cDNA sequence. It covers 2.70 kb, from 208430190 to 208427488 (NCBI 4.1, Aug 2007), on the reverse strand of chromosome 1 (http://www.ncbi.nlm.nih.gov/ieb/research/acembly/av.cgi?db=rat&c=Gene&l=stawflu).

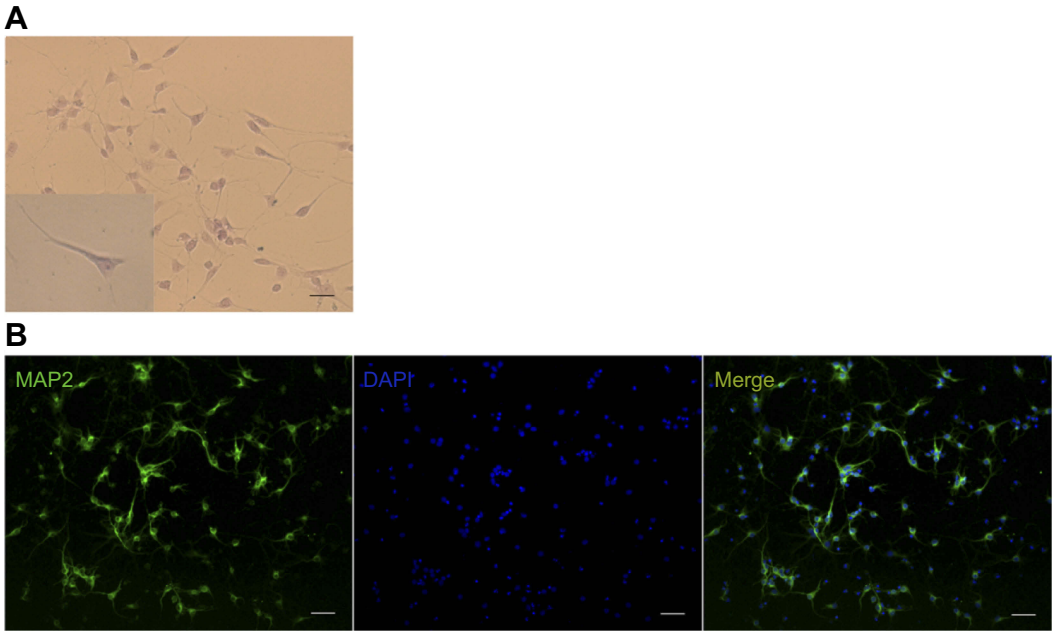

Figure S2 Nissles' stain and immunofluorescence test of neurons in vitro. (**A**) Nissles' stain of neurons. The typical neuron is shown as a brown triangle. (**B**) Immunofluorescence stain of neurons. Neurons are labeled as green using biomarker microtubule-associated protein-2 (MAP-2). Nuclei are stained blue with DAPI. Scale bar=200 μm.

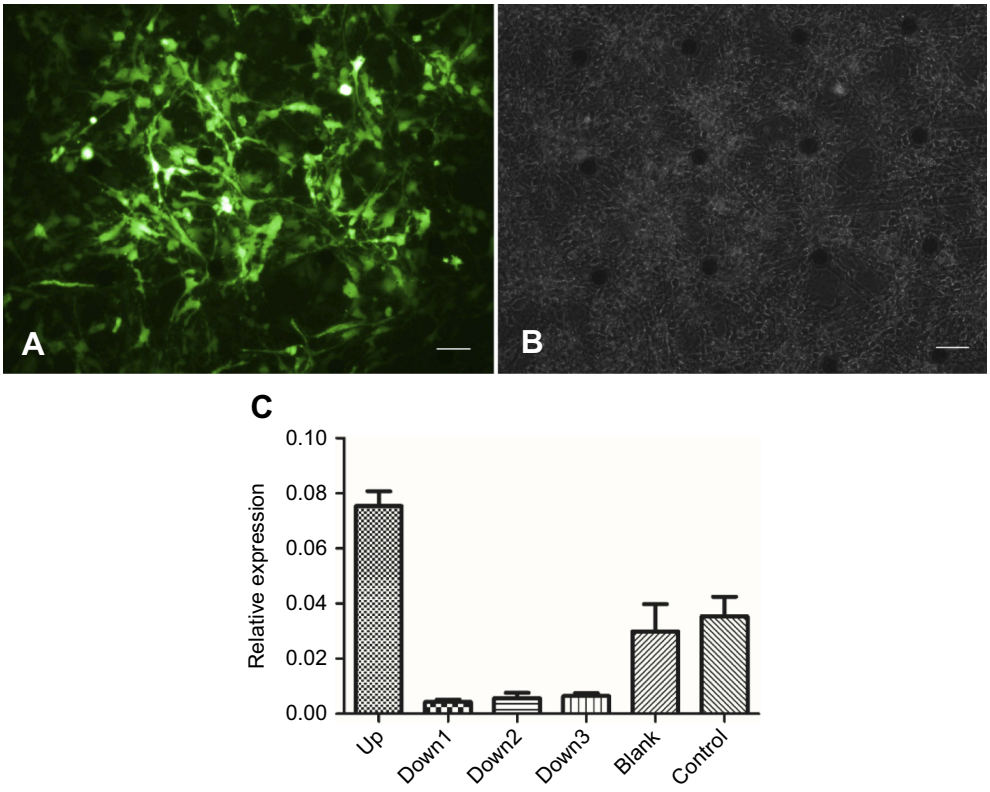

Figure S3 Validation of RNA interference. (**A**) The adenovirus vectors were transfected into neurons and green fluorescent protein was expressed. Scale bar=200 μm. (**B**) The same visual field observed using phase contrast microscope. Scale bar=200 μm. (**C**) Outcome of qRT-PCR for expression of Malat1 after RNA interference. Malat1 upregulated adenovirus was shown in up group. Three Malat1 downregulated adenovirus were shown in down1, down2, and down3 group. The blank group was transferred using adenovirus without interference sequence. The control group was normal neurons. Downregulated adenovirus can effectively decrease the expression of Malat1.

Table S1 The antibodies used in the test of immuno-FISH

Name	Company	Cat. #	Conjugated	Host	Dilution
Anti-NeuN	Abcam	Ab177487	No	Rabbit	1:500
Anti-Iba1	Abcam	Ab5076	No	Goat	1:500
Anti-GFAP	Abcam	Ab7260	No	Rabbit	1:500
Anti-rabbit IgG	Abcam	Ab150129	Alexa fluor 488	Donkey	1:400
Anti-goat IgG	Abcam	Ab150073	Alexa fluor 488	Donkey	1:400

Abbreviations: NeuN, neuronal nuclei; Iba-1, ionized calcium binding adaptor molecule 1; GFAP, glial fibrillary acidic protein.

Table S2 The probes used in the test of immuno-FISH

Name	Tm (°C)	Sequence (5′–3′)	Length	%GC
Malat1-a	66.1	gggccgttataagagtcgactgtcgcatgtacgaaggcatgag	43	53.5
Malat1-b	66.1	gcggttcgttggaggaagctaggaagaaggagccgaaatgatg	43	53.5
Malat1-c	62.4	ggctggtagtttattcttttccccctcccttaacaagacttg	42	45.2
GAPDH	64	cttgtgacaaagtggacattgttgccatcaacgacccccttcattg	45	46.7

Abbreviations: GAPDH, glyceraldehyde phosphate dehydrogenase used as internal control.

Table S3 Target sequence of shRNA used in the synthesis of virus vectors

NO.	Target sequence
Malat1-a	GGTAACATCCCGTGAGGTCGG
Malat1-b	GGGAGTTTGTAGGCTTCTGTC
Malat1-c	GGCGAGCAGGCATTGCGTTGT

Table S4 Sequence of primers used in the synthesis of shRNA

Name	Sequence (5′to 3′)
Malat1a-F(BamHI)	ggatccGGTAACATCCCGTGAGGTCGGTTCAAGAGACCGACCTCACGGGATGTTACCTTTTTTg
Malat1a -R(EcoRI)	gaattcAAAAAAGGTAACATCCCGTGAGGTCGGTCTCTTGAACCGACCTCACGGGATGTTACCg
Malat1b -F(BamHI)	ggatccGGGAGTTTGTAGGCTTCTGTCTTCAAGAGAGACAGAAGCCTACAAACTCCCTTTTTTg
Malat1b -R(EcoRI)	gaattcAAAAAAGGGAGTTTGTAGGCTTCTGTCTCTCTTGAAGACAGAAGCCTACAAACTCCCg
Malat1c -F(BamHI)	ggatccGGCGAGCAGGCATTGCGTTGTTTCAAGAGAACAACGCAATGCCTGCTCGCCTTTTTTg
Malat1c-R(EcoRI)	gaattcAAAAAAGGCGAGCAGGCATTGCGTTGTTCTCTTGAAACAACGCAATGCCTGCTCGCCg